Journal of Pharmacokinetics and Pharmacodynamics (2019) 46:411–426
https://doi.org/10.1007/s10928-019-09634-7

ORIGINAL PAPER

Development and evaluation of a generic population pharmacokinetic model for standard half-life factor VIII for use in dose individualization

Alanna McEneny-King[1] · Pierre Chelle[1] · Gary Foster[2] · Arun Keepanasseril[3] · Alfonso Iorio[3,4] · Andrea N. Edginton[1]

Received: 7 January 2019 / Accepted: 9 April 2019 / Published online: 18 May 2019

Abstract

Hemophilia A is a rare bleeding disorder resulting from a lack of functional factor VIII (FVIII). Therapy consists of replacement with exogenous FVIII, but is complicated by high inter-patient variability. A population pharmacokinetics (PopPK) approach can facilitate the uptake of an individualized approach to hemophilia therapy. We developed a PopPK model using data from seven brands of standard half-life FVIII products. The final model consists of a 2-compartment structure, with a proportional residual error model and between-subject variability on clearance and central volume. Fat-free mass, age, and brand were found to significantly affect pharmacokinetic (PK) parameters. Internal and external evaluations found that the model is fit for Bayesian forecasting and capable of predicting PK for brands not included in the modelling dataset, and useful for determining individualized prophylaxis regimens for hemophilia A patients.

Keywords Population pharmacokinetics · Bayesian forecasting · Hemophilia · Dose individualization

Introduction

Hemophilia A is a genetic bleeding disorder caused by a deficiency of functional clotting factor VIII (FVIII), affecting 1 in 6500 male births [1]. As a result, hemophilia patients are unable to form clots in response to vascular injury and are thus prone to bleeding episodes. Among the most severe patients (i.e. those with less than 1% of normal FVIII activity), bleeds may occur spontaneously, particularly in joints, resulting in debilitating arthropathy. Current hemophilia therapy consists of regular intravenous infusions of exogenous FVIII to maintain FVIII levels above a certain trough at all times. Often, the selected trough is 1% (or 10 IU L^{-1}), based on the observation that the rate of increase in joint score of moderate patients with endogenous FVIII activity between 1 and 3% was halved compared with those with endogenous levels below 1% [2]. Furthermore, a correlation between time spent below the 1% threshold and the occurrences of bleeds and hemarthroses has been demonstrated [3].

Today, there is global consensus that prophylaxis should be initiated at a young age, before joint disease is apparent [4–6]. However, no optimal regimen has been determined due to a highly variable pharmacokinetic (PK) response between patients. High between subject variability (BSV) and relatively low interoccasion variability (IOV) suggests that FVIII dosing regimens ought to be tailored to the individual to ensure both the safety of the patient and the responsible use of expensive clotting factor concentrates [7, 8]. The classic approach to PK-based dose tailoring has been difficult to apply in a clinical setting, especially when using the approach recommended by the International Society of Thrombosis and Haemostasis (ISTH) for bioequivalence studies with new concentrates, which requires more than 10 samples taken over the course of 48 h. More

Electronic supplementary material The online version of this article (https://doi.org/10.1007/s10928-019-09634-7) contains supplementary material, which is available to authorized users.

✉ Andrea N. Edginton
aedginto@uwaterloo.ca

[1] School of Pharmacy, University of Waterloo, Waterloo, ON, Canada

[2] Biostatistics Unit, St. Joseph's Healthcare, Hamilton, ON, Canada

[3] Department of Health Research Methods, Evidence and Impact, McMaster University, Hamilton, ON, Canada

[4] Department of Medicine, McMaster University, Hamilton, ON, Canada

recent ISTH-issued guidelines detail the value of a population pharmacokinetic (PopPK) approach to PK studies oriented to dose individualization [9, 10]. A PopPK model, which provides typical values of PK parameters (e.g. clearance [CL], central volume [V_1]) and quantifies the variability within the population based on patient covariates, can act as informative prior knowledge for the Bayesian estimation of individual PK parameters including half-life and time to target trough.

Several PopPK models for standard half-life (SHL) FVIII products have been published in the literature, and are summarized in Table 1. Each of the cited models is dedicated to one specific brand of FVIII, and FVIII products do vary in ways that may be clinically relevant (Fig. 1). One such characteristic is the source of the FVIII concentrate, which may be plasma-derived (pdFVIII) or recombinant (rFVIII). Plasma-derived concentrates can be further categorized based on their von Willebrand factor (vWF) content: intermediate purity (vWF:FVIII > 1), high purity (vWF:FVIII = 0.2–0.4), or immunopurified (vWF:FVIII < 0.1) [11]. The presence of a native FVIII-vWF complex in pdFVIII has been shown to impact the early phase of the PK profile, but does not appear to affect half-life [12]. Recombinant FVIII products can be classified according to their structure. In 2000, the first B-domain deleted recombinant FVIII product (BDDrFVIII) was released, followed by a B-domain truncated product in 2013 [13]. The purpose of this deletion was to improve production efficiency, with no changes to immunogenicity or pharmacokinetic profile. While some studies have found BDDrFVIII products to be bioequivalent to their full-length counterparts [14–16], others have found that half-lives are shorter after this modification [17, 18]. This may be due to disrupted intermolecular interactions that impact the life span of FVIII [19]. Despite these differences in source and structure, variability seems to be greater across patients than across brands [8]. Thus, a generic PopPK model for SHL FVIII products can be a valuable tool, especially if one considers that hemophilia is a rare disorder with an abundance of similar products, all of which benefit from PK-tailored dosing regimens.

The aim of this study was to develop and evaluate a generic PopPK model for SHL FVIII products, both plasma-derived and recombinant, using data acquired through the Web Accessible Population Pharmacokinetic Service—Hemophilia (WAPPS-Hemo) project. The development of such a model will help to determine if there are distinct PK differences between FVIII brands and the clinical relevance of these differences. Further, the model will be incorporated into the WAPPS-Hemo platform, which tackles the issue of high BSV by using PopPK models for Bayesian forecasting to obtain individual PK estimates from relatively few patient samples. Clinicians provide 2–4 factor levels, along with demographic information, and are provided with individual estimates of relevant PK parameters (such as half-life, time to 1% FVIII activity, or FVIII activity at 72 h). Furthermore, the wide covariate space of the generic model may permit its use for

Table 1 Published PopPK models for standard half-life FVIII products

References	Product	Description
Abrantes [20]	ReFacto AF/Xyntha	2-compartment; combined RUV model; BSV on CL, F and baseline; IOV on CL and V_2; body weight on V_1 and V_2; age, inhibitor status, and study effect on CL; race on V_2; assay on F and RUV
Björkman [21]	Advate	2-compartment; additive RUV model; BSV on CL and V_1; body weight on CL, V_1, and V_2; age on CL
Nestorov [22]	Advate	2-compartment; combined RUV model; BSV on CL and V_1; body weight on V_1; study on proportional error and V_2
Garmann [23]	Kovaltry	2-compartment; combined RUV model; BSV on CL and V_1; lean body weight on CL and V_1
Jimenez-Yuste [24]	NovoEight	1-compartment; combined RUV model; BSV on CL and V; body weight on CL and V; age on CL
Bolon-Larger [25]	Various recombinant and plasma-derived products	2-compartment; proportional RUV model; BSV on CL, V_1 and V_2; HIV status on V_1 [model for continuous infusion]
Karafoulidou [26]	ReFacto	1-compartment; proportional RUV; BSV on CL and V; body weight on CL and V; HIV status on V
Hazendonk [27]	Various recombinant and plasma-derived products	2-compartment; combined RUV; BSV on CL and V_1; age on CL and V_1; blood group and major surgical procedure on CL; product type on F [some continuous infusion patients included]

RUV residual unexplained variability, *BSV* between subject variability, *IOV* inter-occasion variability, *CL* clearance, *F* bioavailability term to account for assay method, V_1 central volume, V_2 peripheral volume

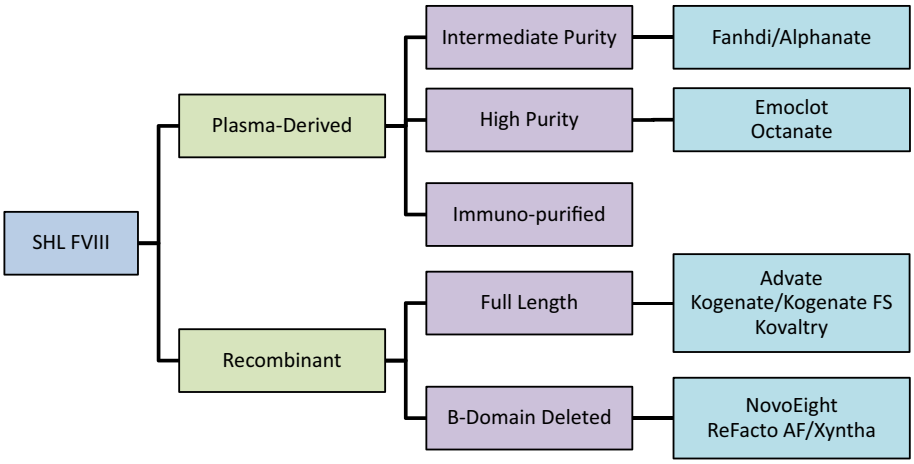

Fig. 1 Sources and structures of the eight brands of SHL FVIII used for model development and evaluation

patients on brands of SHL FVIII that are not included in the modelling dataset, making it particularly useful in cases where a dedicated, brand-specific PopPK model is lacking.

Methods

Patient data

Data for recombinant and plasma-derived SHL FVIII was collected from multiple industry sources through the WAPPS-Hemo project. The model was developed using FVIII activity measurements from 310 densely sampled patients (one infusion per patient), consisting of between 4 and 12 factor levels (median: 10). All samples were measured using the one-stage clotting assay. All patients had either severe or moderate hemophilia (< 1% or 1–5% of normal FVIII activity, respectively) and did not present detectable inhibitors at the time of PK analysis. The lower limit of quantification (LLOQ) varied among studies, ranging between 4 and 12.5 IU L^{-1} (median = 10 IU L^{-1}) and samples that were below limit of quantification (BLQ) comprised 6.9% of the dataset. Demographic details of the modelling dataset can be found in Table 2.

Population modelling

PopPK model building was performed using non-linear mixed effects modelling techniques implemented in NONMEM and PDxPop (v7.3 and v5.2, respectively; ICON Development Solutions, Ellicott City, MD, USA). Graphical analysis was conducted in MATLAB (R2017b, Mathworks, Natick, MA, USA). Samples that were BLQ were handled using the M3 method [28].

Table 2 Demographics of the patient population used to develop the generic SHL FVIII model

Sampling information				
Total number of patients	Total number of samples	Number of BLQ samples (%)	Number of samples per patient	Duration of sampling (h)
310	2760	191 (6.9%)	10 (4–12)	48.0 (3.25–96.25)
Patient demographics				
Brand	*n*	Age (years)	Body weight (kg)	Fat-free mass (kg)
Advate	79	20 (1.1–62)	66.9 (10.6–132.5)	53.5 (8.1–82.7)
Emoclot	14	33 (14–55)	70 (40–93)	55 (35–66.9)
Kogenate	64	19 (5–54)	69.15 (16.6–124.2)	55.4 (14.2–84.3)
Kovaltry	31	31 (12–61)	70 (46–124.2)	53.2 (39.2–76.5)
NovoEight	55	11 (1–54)	42.7 (11.7–107)	35.9 (10–71.4)
Octanate	35	18 (3–54)	53 (18.5–89)	45.8 (14–67.1)
ReFacto AF	32	24 (14–57)	78.5 (50.7–117.2)	59.35 (43.9–75.2)
Total	310	21 (1–62)	66.0 (10.6–132.5)	53.0 (8.1–84.3)

Data reported as median (range) where appropriate

First, the structural component of the model was developed. The model describes not only the exogenous dose administered, but also endogenous FVIII production and any residual FVIII from prior doses as trials did not necessarily include a washout period.

$$C(t) = Ae^{-\alpha t} + Be^{-\beta t} + endogenous\ FVIII + (predose - endogenous)e^{-\beta t}$$

The endogenous FVIII component was considered to be constant; when the endogenous level was unknown or unmeasurable, it was assumed to be half of the LLOQ. Residual exogenous FVIII decayed according to the terminal rate constant; if no predose measurement was taken, it was assumed that there was no exogenous FVIII remaining when the dose was administered. The standard 1- and 2-compartment models were tested. For each, three different residual error models were explored: additive, proportional, and combined additive/proportional.

Following this step, between subject variability (BSV) terms were added to PK parameters using an exponential form. For example:

$$CL_i = CL_{pop} \cdot e^{\eta_i}$$

where CL_i is an individual's clearance, CL_{pop} is the population value for clearance, and η_i is the individual's deviation from population value. The η values follow a normal distribution with a mean of zero, such that the PK parameters are log-normally distributed. Decision-making during these steps was driven by changes in the objective function value (ΔOFV) and shrinkage of the random effects.

The inclusion of explanatory covariates helps to minimize unpredictable BSV. Only covariates that were consistently available for all data sources were investigated; these included body weight, fat-free mass (calculated from body weight, age, and height using the maturation model defined by Al-Sallami et al. [29]), age, and brand. Preliminary covariate analysis consisted of examining plots of η-values versus each covariate. Covariates were then added to the model in a stepwise manner, and either kept or removed based on their effect on OFV, BSV, and parameter estimates. Body weight, fat-free mass, and age were incorporated prior to brand so that demographic differences between datasets were not falsely attributed to brand. Body size metrics were modelled using allometric functions; a variety of functions were considered to model the age effect. Power, linear, and piecewise linear relationships are shown below:

$$CL_i = CL_{pop} \cdot \left(\frac{cov_i}{cov_{med}}\right)^{\theta_{cov-CL}} \cdot e^{\eta_i}$$

$$CL_i = CL_{pop} \cdot \left(1 + \theta_{cov-CL} \cdot \frac{cov_i - cov_{med}}{cov_{med}}\right) \cdot e^{\eta_i}$$

$$CL_i = CL_{pop} \cdot \left(1 + \theta_{cov-CL} \cdot \max\left(0, \frac{cov_i - cov_{med}}{cov_{med}}\right)\right) \cdot e^{\eta_i}$$

where cov_i is the individual's value for the covariate, cov_{med} is the median value for the covariate, and θ_{cov-CL} is the estimated effect of the covariate on CL.

After taking body size and age effects into account, the effect of brand was explored. Initially, each brand was modelled with its own covariate effect either on CL and V_1.

$$CL_i = CL_{pop} \cdot (1 + \theta_{Brand1-CL} \cdot Brand_1) \cdot (1 + \theta_{Brand2-CL} \cdot Brand_2) \cdots \cdot (1 + \theta_{Brand7-CL} \cdot Brand_7) \cdot e^{\eta_i}$$

where $Brand_i = 1$ if the individual was dosed with Brand i; otherwise, $Brand_i = 0$.

Subsequently, brands were grouped together according to results of the previous runs, or based on their source (e.g. plasma-derived, recombinant) and structure (e.g. full-length, B-domain deleted) in an effort to reduce the number of model parameters. Grouping schemes are delineated in Table 3.

Model evaluation

The final SHL FVIII model was evaluated in several steps. First, graphical techniques were employed to assess the model's goodness-of-fit and to assure that all model assumptions were met. Bootstrap analysis was also performed to assess estimated parameters and their associated confidence intervals. One thousand datasets consisting of 310 individuals were generated by randomly sampling the original dataset with replacement; to ensure all groups were represented in the bootstrap datasets, the original dataset was stratified according to age and brand. Parameter estimation was performed for each dataset and the median parameter estimates and corresponding 95% confidence intervals were calculated.

To evaluate the model for use in Bayesian forecasting, internal cross validation and limited sampling analysis were performed. A fivefold cross validation was performed, meaning the dataset was randomly split into 2 subsets, one containing 80% of the data (the learning subset) and the other the remaining 20% (the validation subset). Relative error on individual PK parameters was calculated using the following equation:

$$Relative\ Error = \frac{P_{CV} - P_{full}}{P_{full}}$$

Table 3 Modelling of brand as a covariate

Scheme	Rationale	OFV (ΔOFV)	Reference group	Group details	
1	Individual effect for each brand	25321 (− 89)	Advate	Each brand as its own group	
2	Based on results of Scheme 1	25325 (− 85)	Advate	Effect of Kovaltry removed from CL	
				Effect of Kogenate, NovoEight, and Octanate removed from V_1	
3	Source	25389 (− 21)	Advate	Octanate	
			Kogenate	Emoclot	
			Kovaltry	(Plasma-derived)	
			NovoEight		
			ReFacto AF		
			(Recombinant)		
4	Source and structure	25357 (− 53)	Advate	NovoEight	Emoclot
			Kogenate	ReFacto AF	Octanate
			Kovaltry	(BDD recombinant)	(Plasma-derived)
			(Full-length recombinant)		

OFV objective function value, Δ*OFV* change in OFV compared to model with FFM and AGE

where P_{CV} is the individual parameter estimate (CL, V_1, half-life) obtained during the cross validation using Bayesian forecasting and P_{full} is the "true" value estimated from the initial dataset.

Limited sampling analysis can be used to determine how well the model can predict individual PK parameters from sparse samples. Using a method similar to that described by Brekkan [30], a population of 1000 virtual subjects was generated from the final SHL FVIII model using covariate distributions from the original dataset. For each virtual subject, a treatment regimen corresponding to 50 IU kg^{-1} on a Monday-Wednesday-Friday schedule was simulated for 4 weeks, with the last Friday dose being used for analysis. Different limited sampling schemes consisting of convenient sampling times (e.g. predose, peak, 24 h post-infusion) are described in detail in Table S3; a total of 34 designs were tested. Each design was used to obtain estimates of individual PK parameters using Bayesian forecasting, and estimates from the limited sampling strategies were compared to those obtained from the full sampling design using the following equation:

$$Relative\ Error = \frac{P_{LSS} - P_{full}}{P_{full}}$$

where P_{LSS} is the parameter estimate from the limited sampling strategy and P_{full} is the parameter estimate from the rich sampling design.

External evaluation was performed using data extracted from the WAPPS-Hemo database. Using Bayesian forecasting, PK outcomes including clearance, central volume, half-life, and time with FVIII activity above 2% (TAT2%) were estimated using both the generic SHL FVIII model and a brand-specific model as available on WAPPS. The evaluation dataset was extracted on September 14, 2018 and contained PK for 394 patients on three brands of factor product: Kovaltry (full-length rFVIII), ReFacto AF (BDDrFVIII), and Fanhdi/Alphanate (intermediate purity pdFVIII, not included in the modelling dataset). PK data for Xyntha, a BDDrFVIII product produced using the same manufacturing process as ReFacto AF but calibrated using a different assay, was also included in the evaluation; Xyntha doses were scaled by a factor of 1.38 to account for the difference in calibration, as done in Abrantes et al. [20]. Patients in the validation dataset ranged between < 1 and 78 years of age and weighed between 10.6 and 138.8 kg.

Results

An abridged log of model building steps is found in Table S1. A 2-compartment structure with a combined residual error model and random effects on clearance (CL) and central volume (V_1) was found to be the superior base model; random effects were not included on intercompartmental clearance (Q) or peripheral volume (V_2) due to high shrinkage (> 40%). Of the two body size metrics available, fat-free mass had the strongest correlation with η_{CL} and η_{V_1} (0.558 and 0.808, respectively) and provided the greatest improvement to the model in terms of both OFV (ΔOFV = − 485) and unexplained BSV on CL ($\Delta\omega_{CL}$ = − 10.5%) and V_1 ($\Delta\omega_{V1}$ = − 28.1%). The addition of a fat-free mass effect on V_2 further reduced the

OFV by 116. Based on covariate plots (shown in Fig. S1), the effect of age on CL was explored. Power, linear, and piecewise linear functions for the age effect were investigated. Ultimately, a piecewise linear function with no age effect below the median age was selected.

After accounting for body size and age, there still appeared to be significant differences across brands as shown in Fig. 2. Initially, a unique effect for CL and V_1 was estimated for each brand. In an effort to reduce the number of model parameters, brands were grouped in a number of ways. We began by estimating an individual effect on CL and V_1 for each of the brands included in the dataset, using Advate as the reference brand (Table 3, Scheme 1). Based on the results of this run, effects were either removed (when effect sizes were below 10%) or combined (when effect sizes were within 10% of one another). The brand-specific effects of Kogenate, NovoEight, and Octanate on V_1 were removed, but no brands were similar enough to group (Table 3, Scheme 2). We also explored a grouping scheme based on the source and structure (Table 3, Schemes 3 and 4, respectively) of the factor products. While grouping scheme 2 produced the lowest OFV (25325), grouping scheme 4 was ultimately selected for the final model. This decision was driven by the objective of building a model that can be used for all SHL FVIII products. Since grouping scheme 4 is based on the source and structure of the product, choosing a group for a product not included in the model dataset is intuitive. Although OFV is somewhat increased for this scheme (ΔOFV = + 64), parameter estimates (including BSV) were relatively unchanged. The final model is summarized by the following expression:

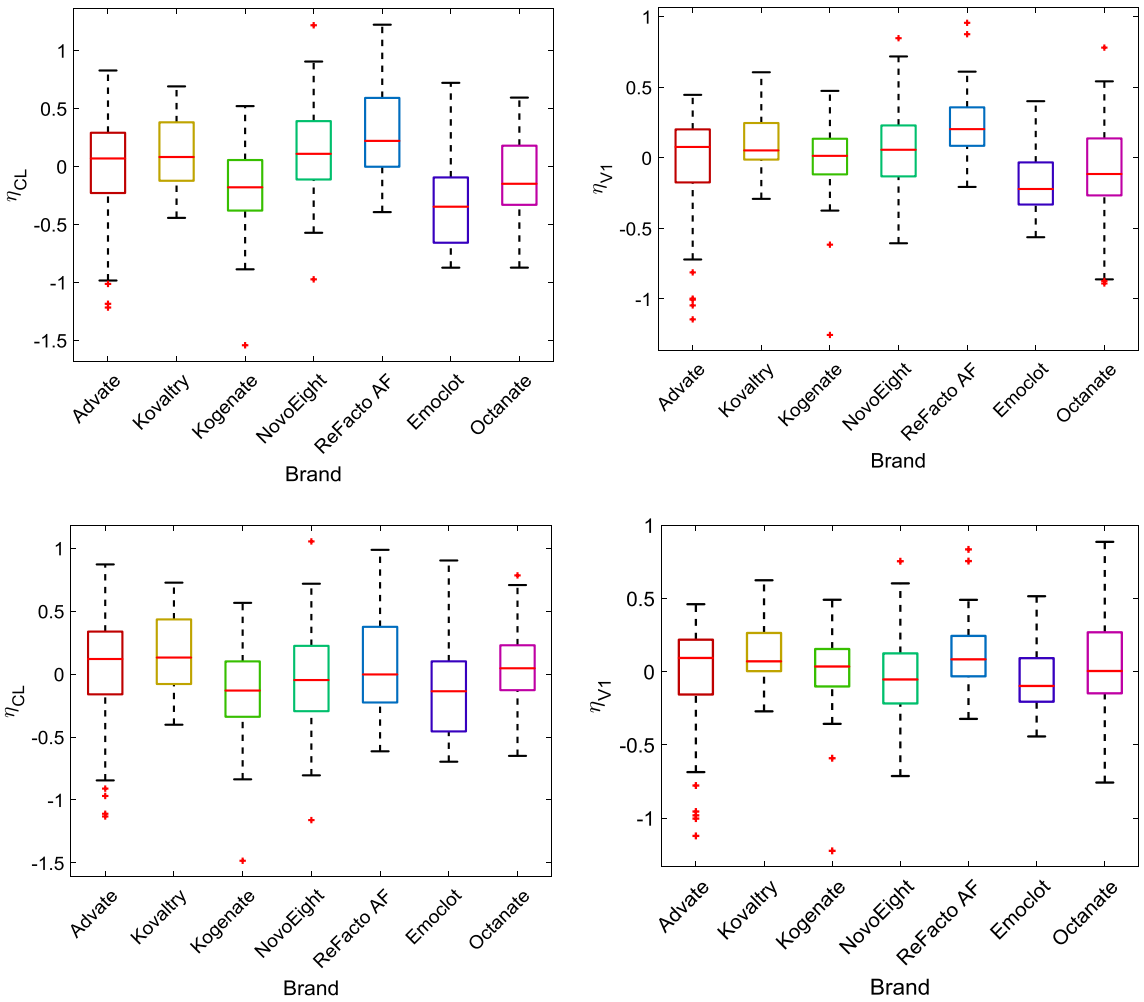

Fig. 2 Boxplots of η-values for clearance (left) and central volume (right) across brands before (top) and after (bottom) inclusion of brand as a covariate

$$\left\{\begin{array}{c} CL = CL_{pop}\cdot\left(\frac{FFM}{53.0}\right)^{\theta_{FFM-CL}}\cdot\left(1+\theta_{AGE-CL}\cdot max\left(0,\frac{AGE-21.0}{21.0}\right)\right)\cdot(1+\theta_{PD-CL}\cdot PD)\cdot(1+\theta_{BDD-CL}\cdot BDD)\cdot e^{\eta_{CL}} \\ V_1 = V_{1pop}\cdot\left(\frac{FFM}{53.0}\right)^{\theta_{FFM-V_1}}\cdot(1+\theta_{PD-V_1}\cdot PD)\cdot(1+\theta_{BDD-V_1}\cdot BDD)\cdot e^{\eta_{V_1}} \\ Q = Q_{pop} \\ V_2 = V_{2pop}\cdot\left(\frac{FFM}{53.0}\right)^{\theta_{FFM-V_2}} \end{array}\right\}$$

where $PD = 1$ for plasma-derived products and $BDD = 1$ for B-domain deleted products.

Goodness-of-fit plots indicate that the model described the data well, with R^2 values of 0.748 and 0.945 for the population and individual predictions, respectively (Fig. 3). Plots of the residual errors suggest that all assumptions of normality are followed, and the pcVPC demonstrates an adequate description of both median values and variability across all time points (Fig. 4). Bootstrap analysis demonstrated the model's stability; RSE % was $\leq$ 30% for all parameters except those associated with the PD brand group (RSE % $\approx$ 50%; Table 4, Fig. S2) and the additive error component ($\geq$ 90%), which was subsequently removed. Internal cross-validation was performed to evaluate the model's utility for Bayesian forecasting. The results summarized in Table S2 and Fig. S3 show low errors (95th percentile of error < 2%) on all parameters of interest (CL, V_1, half-life, and TAT2%). Optimal sampling analysis further evaluated the model's ability to accurately estimate PK parameters from sparsely sampled data. Estimates of half-life and time to 2% (TAT2%) from sampling designs containing 2–3 levels were generally within 15% of those obtained from the rich sampling design (Fig. 5). Errors appear to be largest in sampling schemes that contain only a 72 h point in the tail of the curve, as this sample is likely to be BLQ for a significant proportion of the virtual population. The full results of the optimal sampling analysis can be found in Table S3.

Using data from the 394 patients collected through the WAPPS-Hemo network, we compared the performance of the generic SHL FVIII model to brand-specific models for FVIII products in each of the brand groups of the final model: Kovaltry (full-length rFVIII), ReFacto AF/Xyntha (BDDrFVIII), and Fanhdi/Alphanate (pdFVIII). In each case, Bayesian forecasting produced similar estimates of clearance, central volume, half-life, and TAT2% (Fig. 6) from both models (Kovaltry: $R^2 = 0.94$–0.97; ReFacto AF/Xyntha: $R^2 = 0.86$–0.94; Fanhdi/Alphanate: $R^2 = 0.94$–0.99); the correlation is slightly poorer in the ReFacto AF comparison as the comparator model has a one-compartment structure.

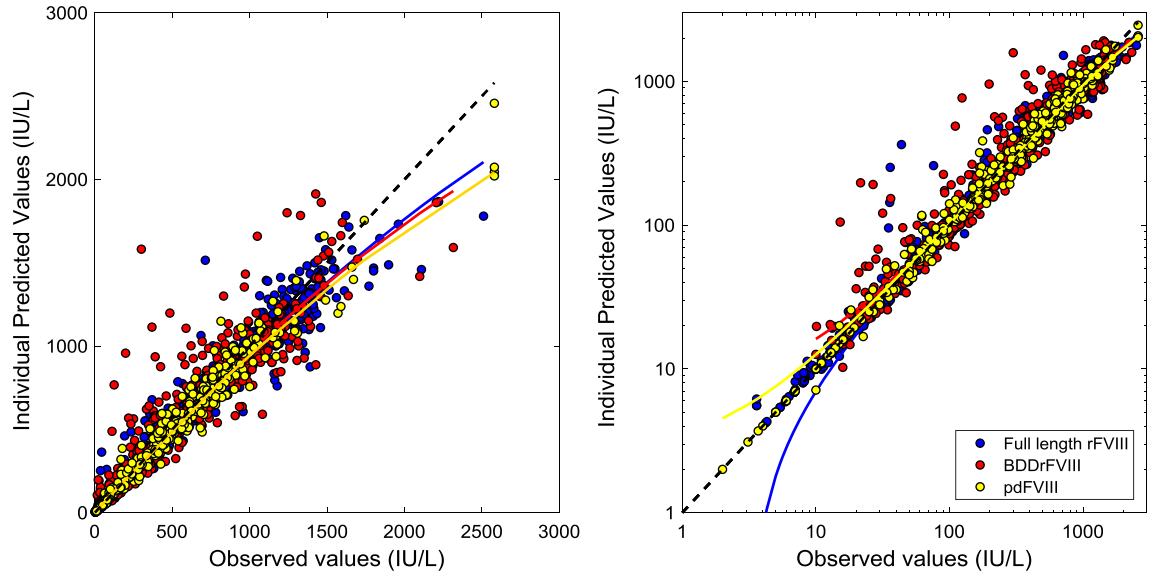

Fig. 3 Individual predicted values from the final SHL FVIIII model versus observed values by brand group on linear (left) and log (right) scale. Samples that were BLQ are not depicted

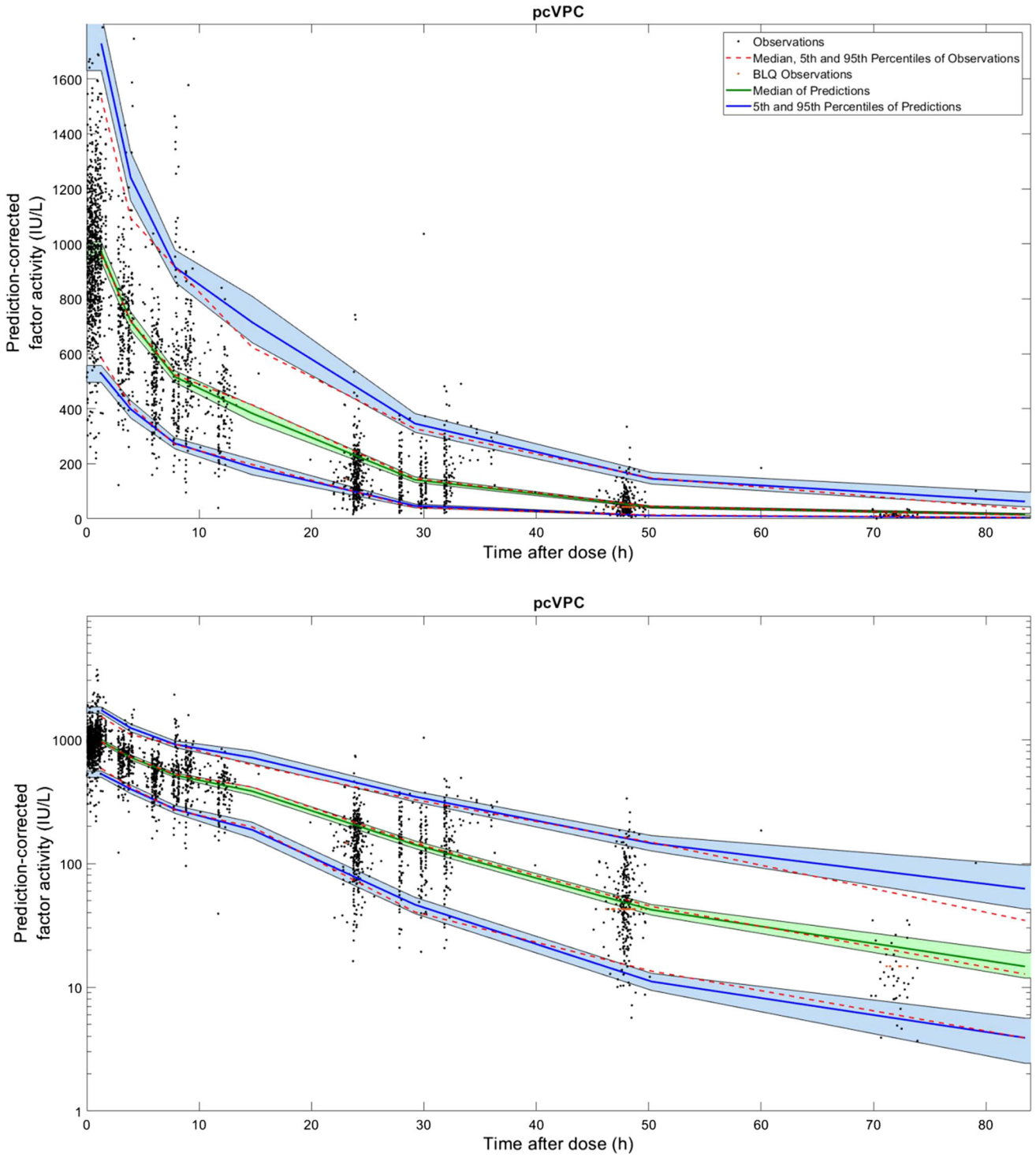

Fig. 4 Prediction-corrected visual predictive check (pcVPC) for the final SHL FVIII model shown on linear (top) and log (bottom) scales. Shaded regions are the 90% confidence intervals for the simulated percentiles

Discussion

This study describes the development and evaluation of a generic PopPK model for SHL FVIII products, built on a dataset containing data measured using the one-stage assay for seven different brands of SHL FVIII. The estimates of population PK parameters were similar to those reported in published brand-specific models despite differences in modelling data, approach, and objective (Table 5). Fat-free mass explained a significant portion of the BSV on CL and

Table 4 Parameter estimates for the final SHL FVIII model

Parameter	Estimate	%RSE	95% confidence interval
Clearance, CL (L h^{-1})	0.238	3.6	(0.221, 0.254)
FFM effect on CL (θ_{FFM-CL})	0.794	6.1	(0.699, 0.883)
Age effect on CL (θ_{AGE-CL})	− 0.205	14.5	(− 0.259, − 0.145)
Central volume, V_1 (L)	3.01	2.5	(2.85, 3.14)
FFM effect on V_1 (θ_{FFM-V_1})	1.02	4.2	(0.940, 1.11)
Intercompartmental clearance, Q (L h^{-1})	0.142	14.4	(0.107, 0.186)
Peripheral volume, V_2 (L)	0.525	7.0	(0.457, 0.600)
FFM effect on V_2 (θ_{FFM-V_2})	0.787	16.5	(0.557, 1.07)
BDD on CL (θ_{BDD-CL})	0.309	23.3	(0.175, 0.461)
BDD on V_1 (θ_{BDD-V_1})	0.159	32.4	(0.060, 0.262)
Plasma-derived on CL (θ_{PD-CL})	− 0.126	54.0	(− 0.232, 0.023)
Plasma-derived on V_1 (θ_{PD-V_1})	− 0.104	52.2	(− 0.195, 0.017)
BSV on CL (%)	41.1%	4.9	(37.3%, 44.9%)
BSV on V_1 (%)	32.4%	7.0	(28.3%, 37.2%)
CL-V_1 correlation	0.703	5.2	(0.624, 0.765)
Proportional error (%)	17.4%	4.8	(16.0%, 19.3%)

V_1 and was likely superior to total body weight due to its better correlation to plasma volume. Age was also found to be a significant covariate for CL, possibly acting as a surrogate for changes in levels of vWF [31], an important predictor of FVIII clearance [32]. It has been shown that vWF levels increase with age in hemophilia A patients [33], resulting in lower clearance and longer half-lives among older patients. The choice of a piecewise linear function to describe this age effect was primarily due to high correlation between FFM and age in children and teenagers. Including both covariates for patients in this age range produces a falsely high estimate of the FFM effect on CL, which in turn results in half-life estimates decreasing when FFM increases. As in the brand-specific models developed for WAPPS-Hemo, the median age (21 years) was selected as the cut-off for the age effect; this value is physiologically plausible, as vWF levels are fairly stable up to this age [33] and the correlation between age and FFM is much weaker after puberty (Fig. S4). Unfortunately, vWF could not be directly included in the model because patient vWF levels were not available for all brands in the modelling dataset; blood group (which can also act as a surrogate for vWF) was also not available consistently and therefore could not be included. However, published models for FVIII that include vWF or blood group as covariates on CL had similar unexplained BSV on CL; moreover, unexplained BSV on CL only decreased by 5–8% after adding vWF or blood group compared to the base or structural model [22, 27]. For the final SHL FVIII model described here, unexplained BSV on CL and V_1 remained high (42% and 31%, respectively) in the final SHL FVIII, even after incorporation of explanatory covariates; one possible explanation for this observation is inter-laboratory variability, as the modelling dataset was compiled from numerous sources. For the one-stage assay, this variability has been estimated to be around 10% for peak levels, but closer to 35% at levels below 50 IU L^{-1} [34–37].

This model was developed with two purposes in mind. First, the model is intended for use in Bayesian analysis to produce accurate estimations of relevant PK parameters from sparse patient data. To evaluate the model for this purpose, fivefold cross-validation and optimal sampling analysis were performed, the results of which indicate the model is well-suited for this purpose. Secondly, it was hoped that by combining data from a variety of SHL FVIII products, we could develop a model that performs Bayesian estimation accurately for all brands of SHL FVIII, including those not included in the modelling dataset. To assess this capability, we compared the estimates of PK parameters for 49 patients on Fanhdi/Alphanate (a plasma-derived SHL FVIII) produced by the generic SHL FVIII model and a dedicated Fanhdi/Alphanate model [38]. Agreement between the estimates from each model was good ($R^2 \geq 0.94$ for $y = x$ regression for all parameters), suggesting that the models produce similar predictions of the parameters of interest. Based on these results, the model seems capable of predicting PK for brands outside the original covariate space, and may prove to be especially valuable for brands for which there is no dedicated PopPK model. An additional strength of the model is the ability to leverage pediatric data from other produts when brand-specific pediatric data is unavailable.

Although it performed well in all evaluations, the model does have some limitations and there may be some instances in which a brand-specific model is more

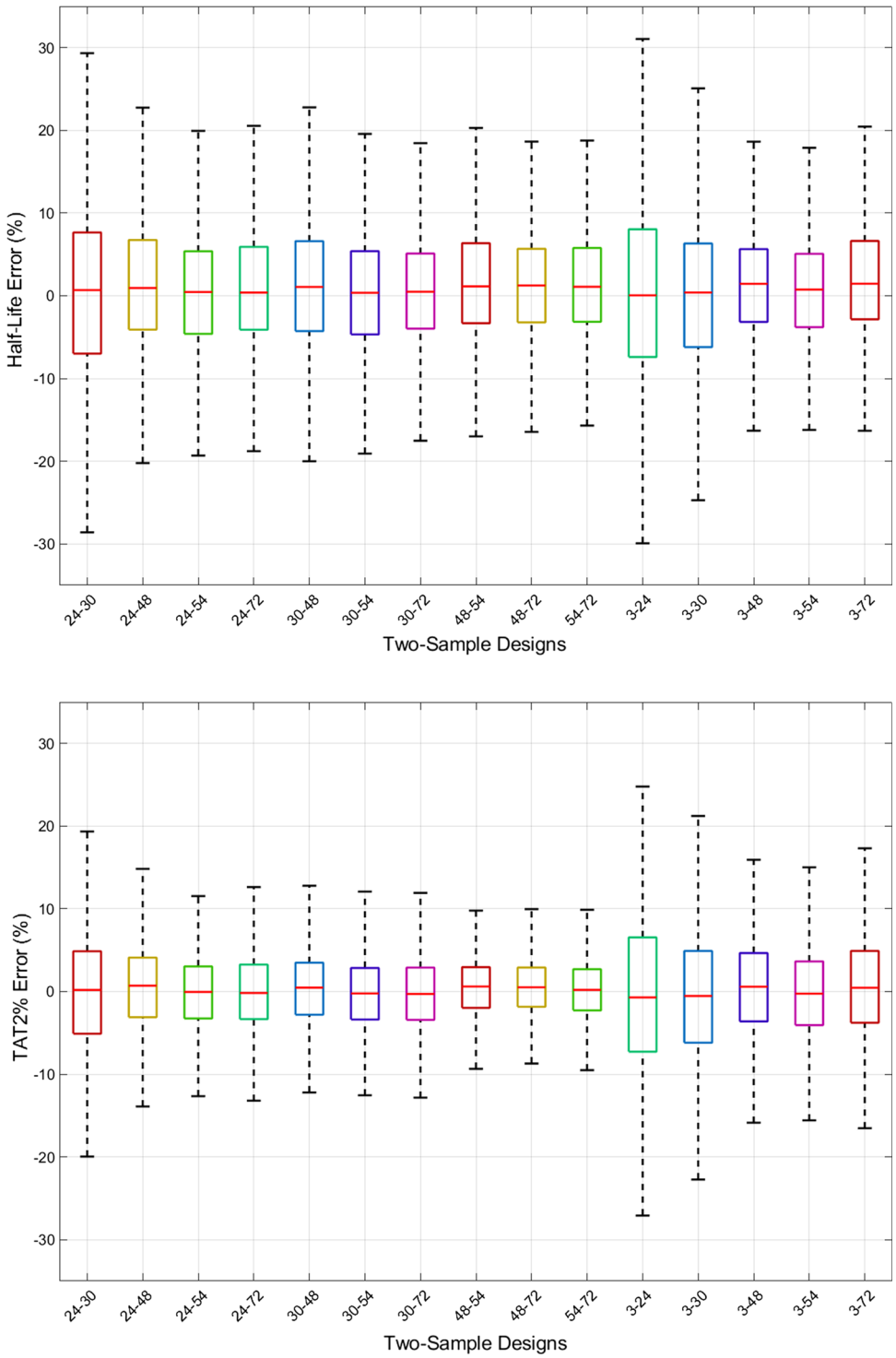

Fig. 5 Errors on estimates of half-life (top) and time to 2% activity (TAT2%, bottom) from limited sampling strategies consisting of 2 post-infusion samples

appropriate. For example, the covariate model of the SHL FVIII model was limited to values that were available across all seven brands. It is well known that additional covariates such as vWF, blood group, and hematocrit can be useful for predicting the PK of FVIII; a brand-specific model may allow for the incorporation of these covariates, resulting in lower unexplained BSV. Additionally, the modelling dataset does not contain pediatric PK data for all of the included brands; NovoEight alone represents over 60% of the data for children under the age of 5. If estimating PK in young patients, a brand-specific model may be preferable, provided that the model is built on enough patients, with an adequate proportion of the data coming from children. On the contrary, the SHL FVIII model

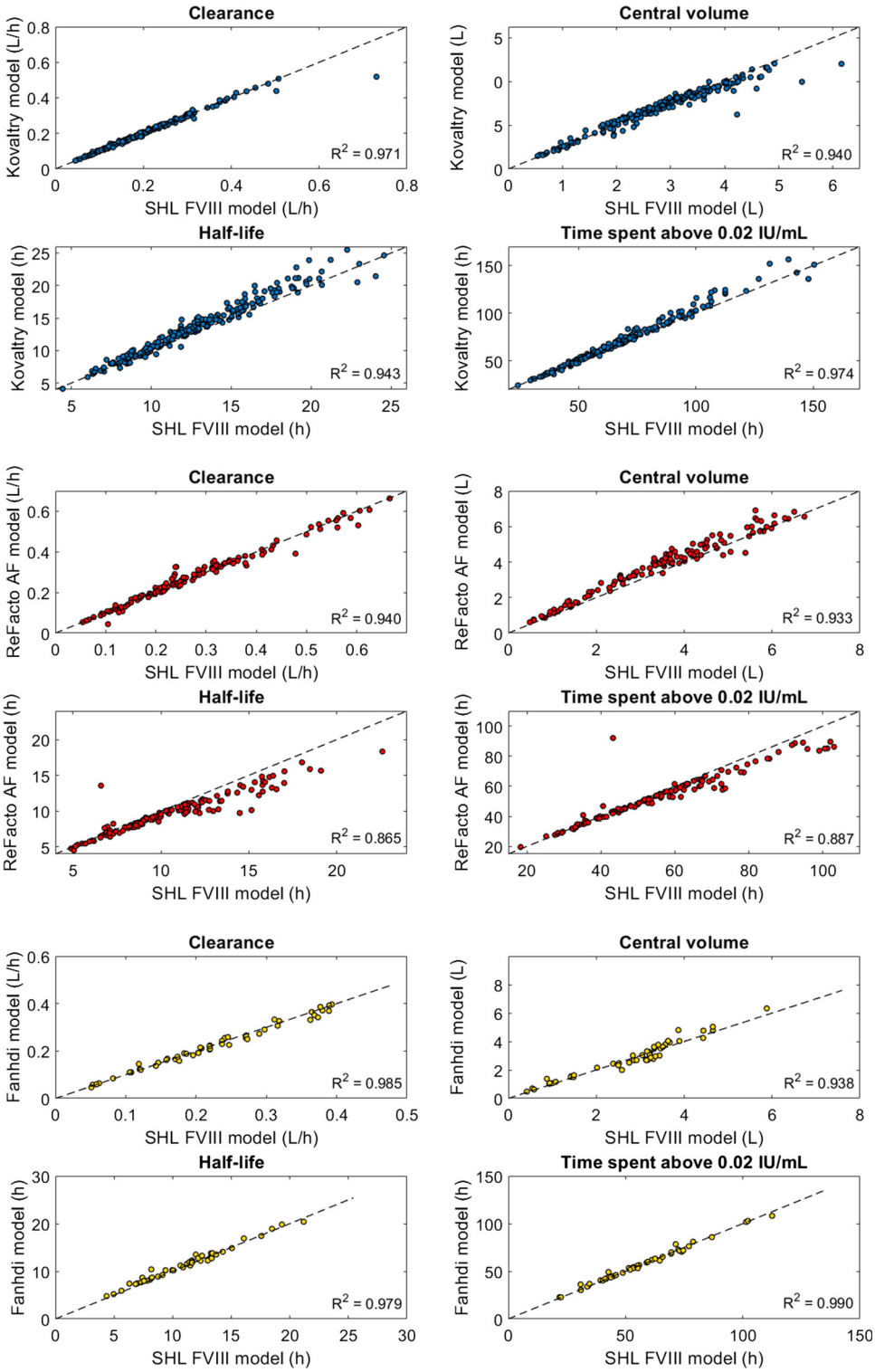

Fig. 6 Comparison of PK parameter estimates generated from the SHL FVIII model and brand specific models for Kovaltry (blue, $n = 213$), ReFacto AF/Xyntha (red, $n = 132$), and Fanhdi/Alphanate (yellow, $n = 49$) (Color figure online)

allows for the leveraging of pooled pediatric data and may prove extremely useful in cases where data in young patients is lacking.

Conclusions

In summary, we have developed a generic PopPK model for plasma-derived and recombinant SHL FVIII products measured using the one-stage assay. Fat-free mass, age, and brand of factor product were found to significantly

Table 5 Summary of parameter estimates from published PopPK models for SHL FVIII

References	Product	Parameter estimates				BSV
		CL (L h^{-1})	V_1 (L)	Q (L h^{-1})	V_2 (L)	
Generic SHL FVIII model	All SHL FVIII products	rFVIII: 0.237 BDDrFVIII: 0.324 pdFVIII: 0.210	rFVIII: 3.00 BDDrFVIII: 4.10 pdFVIII: 2.72	0.143	0.522	[CL] [V_1]
Abrantes [20]	ReFacto AF/Xyntha	0.276	2.45	2.51	0.923	30.5% [CL] 13% [F]
Bjorkman [21]	Advate	0.193	2.22	0.147	0.73	30% [CL] 21% [V_1]
Nestorov [22]	Advate	0.253	3.46	0.055	0.494	30.4% [CL] 16.2% [V_1]
Garmann [23]	Kovaltry	0.188	3.00	0.190	0.637	37.0% [CL] 11.2% [V_1]
Jimenez-Yuste [24]	NovoEight	0.302	3.46	–	–	–
Karafoulidou [26]	ReFacto	0.393	4.86	–	–	38.9% [CL] 13.0% [V_1]

influence PK parameters. All evaluation steps suggest that the model is fit for Bayesian forecasting and capable of accurately predicting individual PK for SHL FVIII, including brands outside the original covariate space.

Acknowledgements We would like to thank the centres in the WAPPS-Hemo network for contributing data used for the external validation of the presented model. The full list of centres is found in Appendix.

Appendix: List of WAPPS-Hemo centres

Alberta Children's Hospital, Calgary, Canada
Amrita Hospital, Kochi, India
Antwerp University Hospital, Edegem, Belgium
AOU Città della Salute e della Scienza di Torino, Turin, Italy
Arthur Bloom Haemophilia centre, Cardiff, United Kingdom
Azienda Ospedaliera Pugliese-Ciaccio, Catanzaro, Italy
Azienda Ospedaliero Universitaria di Parma, Parma, Italy
BC Children's Hospital, Vancouver, Canada
Beijing Children's Hospital, Beijing, China
Belarusian Centre for Paediatric Oncology and Haematology, Minsk, Belarus
Bern University Hospital, Bern, Switzerland
Bloodworks Northwest, Seattle, United States
Calvary Mater Hospital/John Hunter Children's Hospital, Newcastle, Australia
Center for Bleeding and Clotting, Minneapolis, United States
Center for Hemorrhagic and Thrombotic Diseases, University Hospital of Udine, Udine, Italy
Center for Inherited Blood Disorders, Orange County, United States
Centre de traitement des Hémophiles Eaubonne-Montmorency, Montmorency, France
Centre de traitement des Hémophiles Hôpital, Mignot, France
Centre Hospitalier Le Mans, Le Mans, France
Centro Asistencial Regional de Hemoterapia (CARDHE), Bahia Blanca, Argentina
Centro de Hemoterapia e Hematologia do Espirito Santo, Victoria, Brazil
Centro Emofilia di Padova, Padova, Italy
Centro Emofilia e Trombosi, Bari, Italy
Centro Hospitalar de Lisboa Central, Lisbon, Portugal
Centro Médico Imbanaco, Cali, Colombia
Centro. Nacional de Hemofilia, Caracas, Venezuela
CHEO Research Institute, Ottawa, Canada
Children's Hospital Colorado Anschutz Medical Campus, Aurora, United States
Children's Hospital of Michigan, Detroit, United States
Children's Hospital, Boston, United States
Children's Hospital, Los Angeles, United States
Children's Medical University Hospital, Riga, Latvia
Children's of Minnesota, Minneapolis, United States
CHR de la Citadelle, Liège, Belgium
Christchurch Hemophilia Treatment Centre, Christchurch, New Zealand
CHRU de Besançon, Besançon, France
CHU Caen, Caen, France
CHU de Rouen, Rouen, France
CHU Sainte Justine, Montreal, Canada

CHU, University Hospital of Nancy, Nancy, France
Clinique Vasculaire et Coagulation, Angers, France
Complejo Asistencial Dr. Sótero del Río, Santiago, Chile
Complejo Hospitalario de Navarra, Pamplona, Spain
Congenital Coagulopathies Unit, Balearic Islands, Spain
CTH-Cordoba, Cordoba, Argentina
Dr. von Haunersches Kinderspital, Munich, Germany
Ege University Hospital, Izmir, Turkey
Emory University, Atlanta, United States
Erasmus MC, Sophia Children's Hospital, Rotterdam, Netherlands
Exeter and Barnstaple Haemophilia Centre, Barnstaple, United Kingdom
Farwaniya General Hospital, Al Farwaniyah, Kuwait
Fondazione IRCCS Policlinico San Matteo, Pavia, Italy
Fondazione Policlinico universitario "Agostino Gemelli", Rome, Italy
Foothills Medical Centre, Calgary, Canada
Fundación de Hemofilia de Salta, Salta, Argentina
Fundacion de la Hemofilia Rosario, Rosario, Argentina
Fundacion de la Hemofilia, Buenos Aires, Argentina
Gent University Hospital, Gent, Belgium
Gulf States Hemophilia, Houston, United States
Haematology and Haemophilia Centre Catelfranco Veneto, Catelfranco Veneto, Italy
Haemophilia Centre Copenhagen, Copenhagen, Denmark
Haemophilia Centre of Perugia, Perugia, Italy
Haemophilia Comprehensive Care Ljubljana, Ljubljana, Slovenia
Hamilton Health Sciences, Hamilton, Canada
Hämophilie-Zentrum Rhein Main GmbH, Frankfurt, Germany
Heim Pál Gyermekkórház, Budapest, Hungary
Helsinki University Hospital, Helsinki, Finland
Hematologia y oncologia del oriente SAS, Bogota, Colombia
Hematology and Oncology Department, CHU Nord, St. Etienne, France
Hemocentro Unicamp, São Paulo, Brazil
Hemofiliecentrum, UZ Leuven, Leuven, Belgium
Hemophilia Center of Western New York, Buffalo, United States
Hemophilia Center of Western Pennsylvania, Pittsburgh, United States
Hemophilia Comprehensive Care Team, Jakarta, Indonesia
Hemophilia Treatment Center of Central PA, Hershey, United States
Hemostasis and Thrombosis Center of Nevada, Las Vegas, United States
Hemostasis and Thrombosis Center Rhode Island, Rhode Island, United States
Hôpital de l'Enfant-Jésus, Quebec City, Canada
Hôpital Trousseau, CHRU de Tours, Tours, France
Hôpital Universitaire des Enfants Reine Fabiola, Huderf, Belgium
Hôpitaux Universitaires de Genève, Geneva, Switzerland
Hospital Alvaro Cunqueiro, Vigo, Spain
Hospital Clinico Universitario de Santiago, Santiago, Spain
Hospital de la Santa Creu i Sant Pau, Barcelona, Spain
Hospital de Santa Maria, Lisbon, Portugal
Hospital General Universitario de Alicante, Alicante, Spain
Hospital Humberto Notti, Mendoza, Argentina
Hospital Miguel Servet, Zaragoza, Spain
Hospital Posadas, Buenos Aires, Argentina
Hospital Regional Universitario de Málaga, Málaga, Spain
Hospital Roberto del Río, Santiago, Chile
Hospital Sant Joan de Déu, Barcelona, Spain
Hospital Teresa Herrera Materno Infantil, Coruna, Spain
Hospital Universitario Dr José Eleuterio Gonzalez, Monterrey, Mexico
Hospital Universitario La Paz, Madrid, Spain
Hospital Universitario Virgen de la Arrixaca, Murcia, Spain
Hospital University and Politechnic La Fe, Valencia, Spain
Hospital Vall d'Hebron, Barcelona, Spain
Hospital Virgen de las Nieves, Granada, Spain
Hull and East Yorkshire Hospitals NHS Trust, Hull, United Kingdom
Indiana Hemophilia and Thrombosis Center, Indianapolis, United States
Institute of Hematology and Blood Diseases Hospital Chinese Academy of Medical Science, Tianjin,
China
Instituto Guatemalteco de Seguridad Social, Guatemala City, Guatemala
Intergral Solutions SD S.A.S, Bogota, Colombia
IPS Especializada, Bogota, Colombia
IWK Health Centre, Halifax, Canada
Johns Hopkins All Children's Hospital, St. Petersburg, United States
Kaohsiung Medical University Hospital, Kaohsiung, Taiwan
King Faisal Specialist Hospital and Research Centre, Riyadh, Saudi Arabia
Kingston General Hospital, Kingston, Canada
Klinik für Kinder- und JugendmedizinUniversitätsklinikum Jena, Jena, Germany
Korea Hemophilia Foundation Seoul Clinic, Seoul, South Korea
Kuopio University Hospital, Kuopio, Finland
Kyung Hee University Hospital at Gangdong, Seoul, South Korea
Laiko General Hospital of Athens, Athens, Greece
L'hemostase de Strasbourg, Strasbourg, France
London Health Sciences Center, London, Canada
Luzerner Kantonsspital, Lucerne, Switzerland
Manitoba Health Sciences Centre, Winnipeg, Canada
Massachusetts General Hospital, Boston, United States
Maxima Medisch Centrum, Veldhoven, Netherlands
Mohács Hospital, Mohács, Hungary
Montreal Children's Hospital, Montreal, Canada
Nagoya University Hospital, Nagoya, Japan
Nanfang Hospital, Guangzhou, China
National Haemophilia Center Budapest, Budapest, Hungary
Nationwide Children's Hospital, Columbus, United States
Nemours Children's Specialty Care, Jacksonville, United States
North Dakota Hemostasis and Thrombosis Treatment Center, Fargo, United States
North Estonia Medical Center, Tallinn, Estonia

Northern Alberta Bleeding and Rare Blood Disorders Clinic - Kaye Edmonton Clinic, Edmonton, Canada

Northwest Ohio Hemophilia Treatment Center, Toledo, United States

Ogikubo Hospital, Tokyo, Japan

Oklahoma Center for Bleeding and Clotting Disorders, Oklahoma City, United States

ONCOORIENTE SAS, Villavicencio, Colombia

Oregon Health and Science University, Portland, United States

Orthopaedic Hemophilia Treatment Center, Los Angeles, United States

Ospedale S. Bortolo, Vicenza, Italy

Oulu University Hospital, Oulu, Finland

Palmetto Health Richland, Columbia, United States

Pediatric Hemophilia Center of Turin, Italy

Peking Union Medical College Hospital, Beijing, China

Phoenix Children's Hospital, Phoenix, Unites States

Policlinico di Palermo, Palermo, Italy

Policlinico Umberto I - "Sapienza" Università di Roma, Rome, Italy

Pontificia Universidad Católica de Chile, Santiago, Chile

Rady Children's Hospital, San Diego, United States

Riley Children's Health, Indianapolis, United States

Royal Adelaide Hospital, Adelaide, Australia

Royal Brisbane and Women's Hospital, Brisbane, Australia

Royal Free Hospital, London, United Kingdom

Royal London, London, United Kingdom

Ruan Rehacer IPS, Bogota, Colombia

Rush University Medical Center, Chicago, United States

Sahlgrenska University Hospital, Gothenburg, Sweden

Saskatchewan Bleeding Disorders Program, Saskatoon, Canada

Sheffield Children's Hospital, Sheffield, United Kingdom

SickKids Hospital, Toronto, Canada

Skåne University Hospital, Malmö, Sweden

South Texas Hemophilia Treatment Center, San Antonio, United States

St. George's University Hospital, London, United Kingdom

St. Joseph's Hospital - Center for Bleeding and Clotting Disorders, Tampa, United States

St. Jude Affiliate Clinic at NH Hemby Children's Hospital, Charlotte, United States

St. Jude Children's Research Hospital, Memphis, United States

St. Michael's Hospital, Toronto, Canada

St. Paul's Hospital, Vancouver, Canada

St-Luc University Hospital, Brussels, Belgium

Stollery Children's Hospital, Edmonton, Canada

Taichung Veterans General Hospital, Taichung, Taiwan

Taipei Medical University Hospital Hemophilia Center, Taipei, Taiwan

Tampere University Hospital, Tampere, Finland

The Alfred Hospital, Melbourne, Australia

The Bleeding and Clotting Disorders Institute, Peoria, United States

The Children's Hospital at Montefiore, New York, United States

The Children's Hospital of Philadelphia, Philadelphia, United States

The Children's Hospital, Zhengjiang University School of Medicine, Hangzhou, China

The Maine Hemophilia and Thrombosis Center, Scarborough, United States

The Royal Children's Hospital, Melbourne, Australia

The Women's and Childrens Hospital, Adelaide, Australia

Turku University Hospital, Turku, Finland

U.O. Pediatria Generale e Specialistica "B. Trambusti", Bari, Italy

UHHS Cleveland. University Hospitals Health System, Cleveland, United States

Universitaets - Kinderklinik Wien, Vienna, Austria

Universitätsklinikum Bonn, Bonn, Germany

University Children's Hospital Berne, Berne, Switzerland

University Children's Hospital Zurich, Zurich, Switzerland

University Hospital Bristol, Bristol, United Kingdom

University Hospital Brno, Brno, Czech Republic

University Hospital Coventry and Warwickshire, Coventry, United Kingdom

University Hospital Magdeburg, Magdeburg, Germany

University Hospital Southampton, Southampton, United Kingdom

University Hospitals of Leicester, Leicester, United Kingdom

University Medical Center Utrecht, Utrecht, Netherlands

University Medical Centre Ljubljana, Ljubljana, Slovenia

University of California San Francisco Pediatric Hemophilia Treatment Center, San Francisco, United

States

University of Debrecen, Debrecen, Hungary

University of Florida Hemophilia Treatment Cente, Gainsville, United States

University of Helsinki and Children's Hospital, Helsinki, Finland

University of Iowa Children's Hospital, Iowa City, United States

University of Kentucky Hemophilia Treatment Center, Lexington, United States

University of Louisville, Louisville, United States

University of Miami Hemophilia Treatment Center, Miami, United States

University of North Carolina, Chapel Hill, United States

University of Szeged, Szeged, Hungary

University of Virginia Health System, Charlottesville, United States

University of Wisconsin Comprehensive Program for Bleeding Disorders, Madison, United States

Valley Children's Healthcare, Madera, United States

Vanderbilt University Medical Center, Nashville, United States

Vivantes Clinic in Friedrichshain, Berlin, Germany

Wake Forest University, Winston-Salem, United States

Weill Cornell Medical College, New York, United States

Zurich University Hospital, Zurich, Switzerland

References

1. Stonebraker JS, Bolton-Maggs PHB, MichaelSoucie J, Walker I, Brooker M (2010) A study of variations in the reported haemophilia A prevalence around the world. Haemophilia 16(1):20–32
2. Ahlberg Å (1965) Incidence, treatment and prophylaxis of arthropathy and other musculo-skeletal manifestations of haemophilia A and B. Acta Orthop Scand 36(sup77):3–132
3. Collins PW et al (2009) Break-through bleeding in relation to predicted factor VIII levels in patients receiving prophylactic treatment for severe hemophilia A. J Thromb Haemost 7:413–420
4. Oldenburg J (2011) Prophylaxis in bleeding disorders. Thromb Res 127:S14–S17
5. Berntorp E, Spotts G, Patrone L, Ewenstein B (2014) Advancing personalized care in hemophilia A: ten years’ experience with an advanced category antihemophilic factor prepared using a plasma/albumin-free method. Biol Targets Ther 8:115
6. Fischer K, Collins PW, Ozelo MC, Srivastava A, Young G, Blanchette VS (2016) When and how to start prophylaxis in boys with severe hemophilia without inhibitors: communication from the SSC of the ISTH. J Thromb Haemost 14(5):1105–1109
7. Björkman S, Folkesson A, Jönsson S (2009) Pharmacokinetics and dose requirements of factor VIII over the age range 3–74 years. Eur J Clin Pharmacol 65(10):989–998
8. McEneny-King A, Iorio A, Foster G, Edginton AN (2016) The use of pharmacokinetics in dose individualization of factor VIII in the treatment of hemophilia A. Expert Opin Drug Metab Toxicol 12(11):1313–1321
9. Iorio A, Blanchette V, Blatny J, Collins P, Fischer K, Neufeld E (2017) Estimating and interpreting the pharmacokinetic profiles of individual patients with hemophilia A or B using a population pharmacokinetic approach: communication from the SSC of the ISTH. J Thrombs Haemost 15(12):2461–2465
10. Iorio A et al (2018) Performing and interpreting individual pharmacokinetic profiles in patients with Hemophilia A or B: rationale and general considerations. Res Pract Thromb Haemost 2(3):535–548
11. Samor B, Michalski C, Brandin M-P, Andre M-H, Chtourou S, Tellier Z (2012) A qualitative and quantitative analysis of von Willebrand factor contained in a very high-purity plasma-derived FVIII concentrate. Vox Sang 103(1):35–41
12. Morfini M, Marchesini E, Paladino E, Santoro C, Zanon E, Iorio A (2015) Pharmacokinetics of plasma-derived vs. recombinant FVIII concentrates: a comparative study. Haemophilia 21(2):204–209
13. Cafuir LA, Kempton CL (2017) Current and emerging factor VIII replacement products for hemophilia A. Ther Adv Hematol 8(10):303–313
14. Di Paola J et al (2007) ReFacto®1and Advate®2: a single-dose, randomized, two-period crossover pharmacokinetics study in subjects with haemophilia A. Haemophilia 13(2):124–130
15. Recht M et al (2009) Clinical evaluation of moroctocog alfa (AF-CC), a new generation of B-domain deleted recombinant factor VIII (BDDrFVIII) for treatment of haemophilia A: demonstration of safety, efficacy, and pharmacokinetic equivalence to full-length recombinant factor V. Haemophilia 15(4):869–880
16. Kessler CM et al (2005) B-domain deleted recombinant factor VIII preparations are bioequivalent to a monoclonal antibody purified plasma-derived factor VIII concentrate: a randomized, three-way crossover study. Haemophilia 11(2):84–91
17. Gruppo RA, Brown D, Wilkes MM, Navickis RJ (2003) Comparative effectiveness of full-length and B-domain deleted factor VIII for prophylaxis–a meta-analysis. Haemophilia 9(3):251–260
18. Johnston A (2012) The relevance of factor VIII (FVIII) pharmacokinetics to TDM and hemophilia a treatment: is B domain-deleted FVIII equivalent to full-length FVIII? Ther Drug Monit 34(1):110–117
19. Pipe SW (2009) Functional roles of the factor VIII B domain. Haemophilia 15(6):1187–1196
20. Abrantes J, Nielsen E, Korth-Bradley J, Harnisch L, Jönsson S (2017) Elucidation of factor VIII activity pharmacokinetics: a pooled population analysis in patients with hemophilia a treated with moroctocog alfa. Clin Pharmacol Ther 102(6):977–988
21. Björkman S (2012) Population pharmacokinetics of recombinant factor VIII: the relationships of pharmacokinetics To Age and Body Weight. Blood 119(2):612–618
22. Nestorov I, Neelakantan S, Ludden TM, Li S, Jiang H, Rogge M (2015) Population pharmacokinetics of recombinant factor VIII Fc fusion protein. Clin Pharmacol Drug Dev 4(3):163–174
23. Garmann D, McLeay S, Shah A, Vis P, MaasEnriquez M, Ploeger BA (2017) Population pharmacokinetic characterization of BAY 81-8973, a full-length recombinant factor VIII: lessons learned—importance of including samples with factor VIII levels below the quantitation limit. Haemophilia 23(4):528–537
24. Jiménez-Yuste V et al (2015) The pharmacokinetics of a B-domain truncated recombinant factor VIII, turoctocog alfa (NovoEight®), in patients with hemophilia A. J Thromb Haemost 13(3):370–379
25. Bolon-Larger M, Bressolle F, Chevalier Y, Chamouard V, Gomeni R, Boulieu R (2015) Population pharmacokinetics of continuous infusion of factor VIII in hemophilia-a patients undergoing orthopedic surgery. IJPPS 7(2):109–114
26. Karafoulidou A et al (2009) Population pharmacokinetics of recombinant factor VIII: C (ReFacto) in adult HIV-negative and HIV-positive haemophilia patients. Eur J Clin Pharmacol 65(11):1121–1130
27. Hazendonk H et al (2016) A population pharmacokinetic model for perioperative dosing of factor VIII in hemophilia A patients. Haematologica 101(10):1159–1169
28. Beal SL (2001) Ways to fit a PK model with some data below the quantification limit. J Pharmacokinet Pharmacodyn 28(5):481–504
29. Al-Sallami HS, Goulding A, Grant A, Taylor R, Holford N, Duffull SB (2015) Prediction of fat-free mass in children. Clin Pharmacokinet 54(11):1169–1178
30. Brekkan A, Berntorp E, Jensen K, Nielsen EI, Jönsson S (2016) Population pharmacokinetics of plasma-derived factor IX: procedures for dose individualization. J Thromb Haemost 14(4):724–732
31. Konkle B (2014) von Willebrand factor and aging. Semin Thromb Hemost 40(06):640–644
32. Lenting PJ, Van Schooten CJM, Denis CV (2007) Clearance mechanisms of von Willebrand factor and factor VIII. J Thromb Haemost 4(7):1353–1360
33. Lalezari S et al (2014) Correlation between endogenous VWF: Ag and PK parameters and bleeding frequency in severe haemophilia A subjects during three-times-weekly prophylaxis with rFVIII-FS. Haemophilia 20(1):e15–e22
34. Turecek PL et al (2016) A world-wide survey and field study in clinical haemostasis laboratories to evaluate FVIII: C activity assay variability of ADYNOVATE and OBIZUR in comparison with ADVATE. Haemophilia 22(6):957–965
35. Barrowcliffe TW (2003) Standardization of FVIII & FIX assays. Haemophilia 9(4):397–402
36. Sommer JM et al (2014) Comparative field study evaluating the activity of recombinant factor VIII Fc fusion protein in plasma samples at clinical haemostasis laboratories. Haemophilia 20(2):294–300

37. Viuff D, Barrowcliffe TW, Saugstrup T, Ezban M, Lillicrap D (2011) International comparative field study of N8 evaluating factor VIII assay performance. Haemophilia 17(4):695–702
38. Chelle P et al (2014) Routine clinical care data for population pharmacokinetic modeling: the case for Fanhdi/Alphanate in hemophilia A patients. J Pharmacokinet Pharmacodyn. https://doi.org/10.1007/s10928-019-09637-4